

PROCEEDINGS OF SPIE

SPIDigitalLibrary.org/conference-proceedings-of-spie

Spectral properties of multilayered oak leaves and a camouflage net: experimental measurements and mathematical modelling

Mikkelsen, A., Selj, G.

A. Mikkelsen, G. K. Selj, "Spectral properties of multilayered oak leaves and a camouflage net: experimental measurements and mathematical modelling," Proc. SPIE 11865, Target and Background Signatures VII, 1186505 (12 September 2021); doi: 10.1117/12.2597968

SPIE.

Event: SPIE Security + Defence, 2021, Online Only

Spectral properties of multilayered oak leaves and a camouflage net – experimental measurements and mathematical modelling

A. Mikkelsen,^{a,*} G. K. Selj^a

^aNorwegian Defence Research Establishment, Instituttveien 20, 2007 Kjeller, Norway

ABSTRACT

The development of state-of-the-art surveillance technology forces nations to develop camouflage with advanced capabilities. Owing to the abundance and wide distribution of leaves, their spectral properties are often mimicked by camouflage material to decrease the conspicuity of the user operating in woodland theaters. Before interacting with the covered object or soil, light usually interacts with several leaf layers, for example through tree canopies. Knowledge of the spectral characteristics of multi-layered leaves is therefore essential to utilize remote sensing applications and for the endeavor to develop undetectable camouflage materials mimicking nature. The literature is currently scarce on research investigating both the spectral characteristics of multi-layered leaves and camouflage material. In this work, we intend to reduce the knowledge gap with studies on the spectral properties of multiple layers of oak leaves and a generic camouflage net. We measured the reflectance and transmittance of samples with 1–8 layers between 250–2500 nm and found that wavelengths and samples differ in penetration depths. The penetration depth ranged from just a couple of layers for visible light to tree or six layers at infrared wavelengths for the camouflage net and leaf samples, respectively. Moreover, we fitted the reflectance data of the samples with an uncomplicated plate model, here named the extinction model, which we used at selected wavelengths to estimate the transmittance and absorptance values of the multi-layered samples. The model predicts the spectral values of the samples with high accuracy, especially those of the leaf samples, and proves to be a promising tool that may replace experiments due to time restrictions or limited resources.

Keywords: leaves, spectral imaging, reflectance, transmittance, camouflage materials, mathematical models.

*Alexander Mikkelsen, E-mail: alexander.mikkelsen@ffi.no

1 INTRODUCTION

With the rapid development of modern technology comes modern surveillance systems produced at a lower cost with increased sensitivity and spectral resolution. Eyes, once the sole sensor for visible light detections is now often replaced by advanced sensors able to detect electromagnetic radiation ranging from UV to radio wavelengths. Worldwide proliferation and the enhanced capabilities of sensors have become a challenging security issue for military forces striving to remain undetected. Camouflage counters surveillance by minimizing detectability or recognition by observers and increases chances of survivability on the battlefield. Including humans, there is a plethora of examples in nature where creatures utilize camouflage to shield themselves from predators or to become effective predators themselves[1-3], and we have spent a long time investigating camouflage techniques from nature to copy them for ourselves[4].

Depending on various factors, for instance nationality and theater of operation, there is a large variety of camouflage designs and techniques[5, 6]. A common camouflage approach is to aim for crypsis through background resemblance[7]. Leaves are prominent in woodland theaters around the world. Camouflage material mimicking the solar reflectance of leaves will thus have low contrast with backgrounds in woodland theaters and be a good strategy to counter advanced surveillance systems. Leaves exhibit four basic features in their reflectance spectra: (1) a green peak around 550 nm owing to the absorption of chlorophyll ; (2) a sharp reflectance increase near 680 nm (red edge) stemming from multiple reflections of the leaf cell structure and reduced chlorophyll absorption; (3) an infrared plateau between ~800 – 1300 nm where the reflectance varies little; and (4) distinct water absorption bands in the infrared region around 1450 and 1940 nm[8-11]. Researchers using special pigments in a bionic membrane recently managed to mimic the reflectance spectrum of leaf [12, 13].

In this work, we study the spectral properties of pedunculate oak leaves (*Quercus robur*), widely distributed in Europe, as well as a generic camouflage net. One of the main motivations for the study is to understand the spectral properties of multiple layers (various thicknesses) of oak leaves and typical camouflage. Better insight into the multi-layered behavior of leaves and camouflage material is useful from both a fundamental and practical point of view. In nature, light often interacts with multiple leaves before hitting the soil or a concealed object, e.g. under a tree canopy. To understand canopy reflectance and penetration depth, or to develop camouflage material mimicking woodland backgrounds, the characteristics of multi-layered leaves are key. As an example, selected reflectance bands of canopies are effectively used in remote sensing technology to monitor properties such as vegetation moisture content and quality (i.e. stress, decay stage, chlorophyll content) related to crop production or fire behavior models[14-18]. However, many of the vegetation indices used to estimate these values include wavelengths that can differ in their canopy penetration depths. Without knowledge of the canopy penetration depths, the indices could be inaccurate in places with high canopy depth (large leaf area index).

A camouflage net is a typical camouflage material that is widely used to passively reduce the detectability of soldiers, vehicles, and valuable targets. It is functional, light, relatively cheap, and offers protection over a large range of wavelengths. Over the last decades, various camouflage net functionalities have been developed and researched, including thermal properties[19-21], models for signature prediction[22], propagation of radar wavelengths[23], and their effectiveness in synthetic aperture radar (SAR) images[24]. Apart from our previous work on the reflectance of a multi-layered camouflage net[25], the literature is scarce on the spectral behavior of multilayered camouflage material. A motivation for this study is thus to further the knowledge on multilayered camouflage nets, advancing our previous work to include both reflectance and transmittance measurements. Multilayered systems allow for advanced artificial camouflage, e.g. functional mimicry of natural camouflage such as a chameleon robot[26] or electrically actuated camouflage devices that can modulate their visible and IR specular-to-diffuse transmittance ratios[27]. Modern camouflage nets often consist of multiple layers enabling improved or additional functionalities such as electromagnetic signature control[28, 29], thermal suppression[30], insulation[31, 32], or cooling mechanisms[33-35].

Another motivation for this work is to test an uncomplicated mathematical model for estimating the spectral properties of layered samples. Being able to easily and properly estimate spectral properties of multilayered camouflage material and biomaterials is useful to save both time and resources. Presently there are many advanced leaves models, ranging from plate models to computer-based and ray tracing models[36, 37]. The plate model is a straightforward approach to predict the spectral characteristics of a stack of leaves (or textiles). In the plate model, leaves are modeled as parallel transparent plates and the spectral properties of multiple leaf layers are calculated from the known spectral characteristics of the material constituting the layers. There are different plate models of various complexities, including the models proposed by Stokes[38], Kubelka and Munk[39, 40], Tuckerman[41], Rampton and Grow[42], Schaich[43] and Sokoetsky[44]. Modified models based on these methods have proven useful to estimate the spectral properties of textiles[45, 46] and stacked leaves[25, 47, 48].

In this work, we use a plate model (here named the extinction model) developed by Wilhelm and Smith[45] for multilayered textiles to here estimate the transmittance and absorptance of oak leaf and camouflage net samples. The model was fitted to the measured reflectance data of 1–8 layers of the samples using two fitting parameters: the sample reflectivity and extinction coefficient. The former is the reflectance of the sample when the thickness approaches infinity, while the latter captures the energy absorption of the sample material. The work is a continuation of our previous study where we compared a generic camouflage net to birch leaves and used a simple mathematical plate model to predict the reflectance of the camouflage net material[25]. In contrast to the extinction model used here, the model utilized in our previous work did not include absorption and multiple-scattering effects, and the model was only compared with reflectance measurements.

2 EXPERIMENTAL SETUP AND METHOD

2.1 Spectral measurements

The reflectance and transmittance spectra of the samples were measured by a spectrophotometer (PerkinElmer Lambda 750S UV/VIS/NIR) between 250 and 2500 nm with a 10 nm interval. A deuterium lamp (part. number L6022728, PerkinElmer) and a tungsten lamp (part. number B0114620, PerkinElmer) were used as illuminants between 250–319.2 nm and 319.2–2500 nm, respectively. To imitate the diffuse nature of the radiation illuminating the background through the sample, we used a spectrophotometer with an integrating sphere (60 mm diameter InGaAs integrating sphere, spectralon coating, PerkinElmer part. number L6020203). An overview of the experimental setup is presented in Figure 1. Before each measurement series, we calibrated the spectrophotometer by fixing a white reference plate (PELA9058 - Calibrated white plate, Spectralon®. 2" calibrated diffuse reflectance standard, PerkinElmer) on the reflectance port and by running a calibration program in the instrument software (UV WinLab v. 6.4.0.973). For the transmittance measurements, the reference plate stayed in the reflectance port while a sample was placed at the transmittance port (Figure 1). The reference plate was replaced by samples for the reflectance experiments. All reflectance measurements were performed with a black background (reflectance 4–5 %) placed behind the samples (Figure 1(d)).

We measured the reflectance and transmittance of 1–8 layers of each sample. More than 8 layers did not have any notable effect on the spectral properties of the samples. Each measurement was usually repeated 2–3 times on different samples, e.g. we changed the oak leaves between the repeated measurements. The spectrophotometer saved the spectral data as .txt files that we analyzed and plotted in Origin Pro 2021 (v. 9.8.0.200). All the spectral measurement results presented in this paper are mean values from several measurements.

The oak leaves examined in this study were collected directly from trees in the summer and brought to the laboratory for measurements less than 2 hours later. We kept the leaves in a sealed plastic bag before and between measurements to maintain their water content. By changing samples between measurements, we also reduced moisture loss in the oak leaves caused by radiation. We also studied a generic camouflage net in this paper. The net was perforated, unicolorous and, consisted of a single layer. Before measuring the samples, they were cut in parts of areas around 7x7 cm, i.e. slightly larger than the maximum port opening of the spectrophotometer (5x6 cm). To reduce repetitive effects from overlapping holes of stacked net layers, we randomly oriented each layer of camouflage net between each measurement.

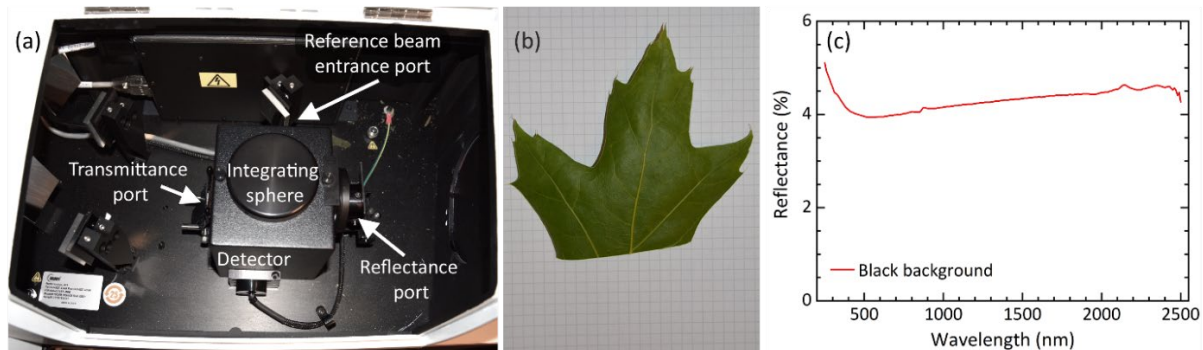


Figure 1. Experimental setup. (a) spectrophotometer (PerkinElmer Lambda 750S UV/VIS/NIR), (b) an oak leaf on 5 mm grid paper, and (c) the background reflectance spectrum. The samples were fastened at the reflectance port for the reflectance measurements and at the transmittance port during the transmittance experiments. A white reference plate (PELA9058 - Calibrated white plate, Spectralon®. 2" calibrated diffuse reflectance standard, PerkinElmer) was placed at the reflectance port during calibration and the transmittance measurements.

2.2 Sample mass per area

We weighted the leaves and net samples on a tabletop scale (TE3102S, Sartorius, readability 0.01 g, reproducibility ± 0.01 g, and linearity ± 0.02 g). The measured samples were then placed on a 5 mm grid paper and photographed from above. To estimate the area of the samples, we analyzed the images in Adobe Photoshop CS6 (v. 13.1.2) and compared the number of pixels in the samples with the number of pixels in the squares on the grid paper. Partial pixel areas (± 3 pixels from the sample selection edge) were estimated to be $\sim 0.8\%$ of the total sample area ($\sim 3.8\text{--}6.5 \times 10^6$ pixels).

Measurement errors due to curvature of the samples and parallax (camera lens and grid paper lines not parallel) were estimated to be less than 3% of the total sample area and less than 0.7% of the measured 1 cm² paper grid area (~0.7–2.7 × 10⁵ pixels). The mean mass per area of each sample was then calculated from the weight and area measurements. Table 1 presents the mean mass (m), area (A), mass per area (m/A) and estimated errors (E) of the oak leaves and net samples. The mass per area values express thicknesses of the samples when used in the extinction model (see Sec. 3).

Table 2. Mean mass (m), area (A), mass per area (m/A) and estimated errors (E) of the oak leaves, and net samples.

| Sample | m (g) | E_m | A (cm ²) | E_A | m/A (mg/cm ²) | $E_{m/a}$ (mg/cm ²) |
|------------|---------|-------|------------------------|-------|-----------------------------|---------------------------------|
| Oak leaves | 0.72 | 0.02 | 43.3 | 1.6 | 16.5 | 0.8 |
| Net | 0.27 | 0.02 | 24.2 | 0.9 | 11.2 | 0.90 |

3 THEORETICAL MODEL

The spectral data in this paper is fitted with a mathematical model, here named the extinction model. In this section, we will introduce the model and show how it can estimate the spectral properties of samples based on multilayered spectral measurements.

3.1 The extinction model

Wilhelm[45] originally derived the extinction model to describe quantitatively the reflectance, transmittance, and absorptance by textiles in terms of specific reflection and absorption characteristics of fibers. The model is based on the Stokes equations[38] for transmittance t_n and reflectance r_n of n plates:

$$t_n = \frac{c-c^{-1}}{cd^n-c^{-1}d^{-n}}, \quad (1)$$

$$r_n = \frac{d-d^{-n}}{cd^n-c^{-1}d^{-n}}, \quad (2)$$

where c and d are constants that only depend on the reflectance and transmittance of the single plates. The equations above were fitted to textile materials of different thicknesses expressed as weight per area by defining $c = 1/\alpha$ and $d = e^k$. Here the constant α is the reflectivity of the material when the thickness goes towards the extreme limit, k the extinction coefficient, while the constant e^{-kw} is the remaining energy fraction after absorption in a unit weight per area w of the material. Substituting n with w , which is the weight per unit area, and using the new definitions yield[45]:

$$t_w = \frac{(1-\alpha^2)e^{-kw}}{1-\alpha^2e^{-2kw}}, \quad (3)$$

$$r_w = \frac{\alpha(1-e^{-2kw})}{1-\alpha^2e^{-2kw}}. \quad (4)$$

The corresponding absorptance is then given by the following relationship: $a_w = 1 - r_w - t_w$.

For semi-transparent samples (such as snow, vegetation, and thin artificial material) we have to account for the optical characteristics of both the i) sample and the ii) underlying background[25, 48]. The spectral characteristics of the background must therefore be included for correct modeling. If the reflectance of the background is given by β , expressions for the reflected, transmitted, and absorbed light of the system (sample and background) is given by[45]:

$$\left(\frac{I_r}{I_0}\right)_{\text{sys.}} = r_w + t_w^2\beta + t_w^2r_w\beta^2 + t_w^2r_w^2\beta^3 + \dots = r_w + \frac{t_w^2\beta}{1-r_w\beta}, \quad (5)$$

$$\left(\frac{I_t}{I_0}\right)_{\text{sys.}} = t_w(1-\beta) + t_w r_w \beta(1-\beta) + t_w r_w^2 \beta^2(1-\beta) + t_w r_w^3 \beta^3(1-\beta) \dots = \frac{t_w(1-\beta)}{1-r_w\beta}, \quad (6)$$

$$\left(\frac{I_a}{I_0}\right)_{\text{sys.}} = 1 - \left(\frac{I_r}{I_0}\right)_{\text{sys.}} - \left(\frac{I_t}{I_0}\right)_{\text{sys.}} = \frac{a_w(1+\beta)(t_w-r_w)}{1-r_w\beta}. \quad (7)$$

4 RESULTS – REFLECTANCE

4.1 Reflectance of multiple layered samples

Figure 2 presents the measured reflectance of 1–8 layers of the oak leaf and the camouflage net samples (for clarity, we do not present all eight layer configurations). The measured reflectance of the oak leaves did not change significantly when increasing the number of layers above a single layer for wavelengths shorter than ~ 720 nm, between ~ 1400 – 1500 nm, and for wavelengths longer than ~ 1880 nm. The reflectance of the oak leaf samples differed most between ~ 800 – 1300 nm. At 900 nm, for example, the measured reflectance of a single layer (red solid line, Fig. 2 (a)) and 8 layers (orange dash-dot-dashed line, Fig. 2 (a)) of oak leaves was 46% and 78%, respectively. For these wavelengths (~ 800 – 1300 nm), the penetration depth of the leaves was 6 layers, i.e. 6 layers of leaves were sufficient to block the reflectance contribution from the black background. More than 6 layers of leaves did not change the reflectance noticeably at any measured wavelengths. Liquid water has absorption peaks of increasing size around 970, 1200 1450, and 1950 nm[49]. These absorption peaks correspond well with the valleys observed in the reflectance spectra of the leaves.

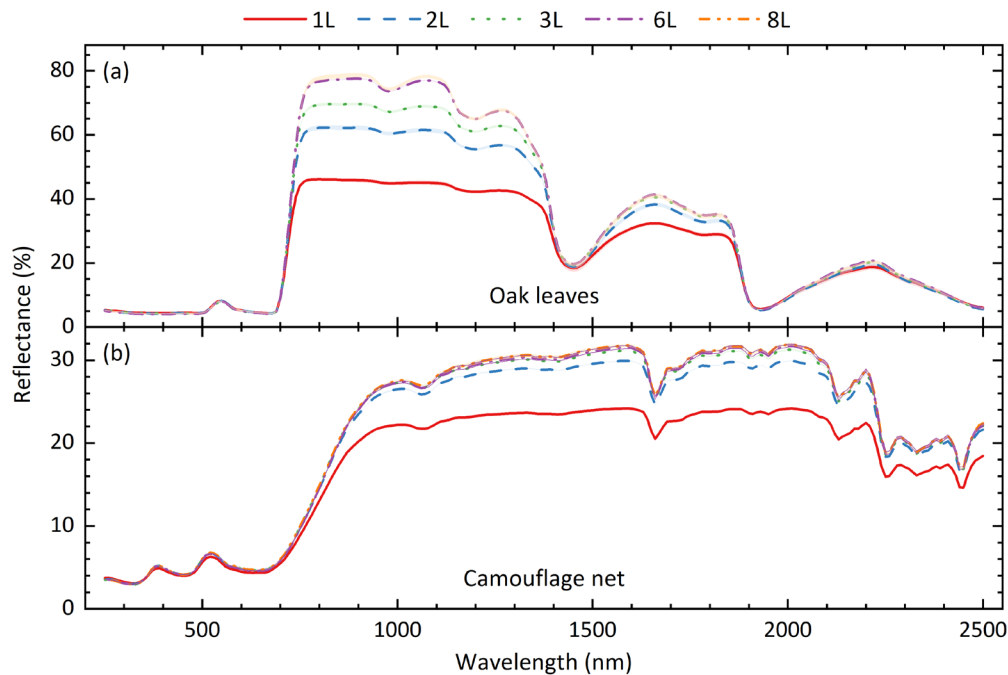


Figure 2. Spectral reflectance measurements of 1 (red solid lines), 2 (blue dashed lines), 3 (green dotted lines), 6 (violet dash-dotted lines) and 8 layers (orange dash-dot-dashed lines) of (a) oak leaves and (b) camouflage net between 250 and 2500 nm. A black background was used for these measurements (reflectance between 4–5%). The shaded bands behind the lines represent the standard error of the reflectance mean (errors smaller than the lines might not be visible in the plot).

For most of the measured wavelengths, the camouflage net Fig. 2 (b) reflected less light than the oak leaves. We also observed that the shape of the reflectance curves differed considerably. For example, the reflectance curve of the net samples did not have such a sharp reflectance increase above 700 nm as the oak leaves. The sharp reflectance increase of leaves is related to their internal structure[9]. We found that the reflectance of the net slightly increased with wavelengths between 800–2200 nm, while the reflectance of the leaves decreased over the same wavelength range. Comparing the reflectance curves of net samples, we observed that 3 layers were sufficient to cancel background reflectance contributions over all wavelengths (Fig. 2 (b)). For wavelengths shorter than ~ 900 nm and larger than ~ 2100 nm, more than 2 layers of the net material did not change the sample reflectance. This indicates that the camouflage net was less transparent and/or absorptive than the oak leaves, and that fewer layers are required to hide the reflectance signature from any object underneath. Note that the reflectance of the sample material, i.e. the samples' reflectivity, is found when the sample thickness goes towards infinity. For thin samples, the reflectance measured by the spectrophotometer contains reflected light from both the sample and the background. If the reflectivity of the background is very different from that of the sample, the measured reflectance will also change markedly with sample thickness.

4.2 Fitting the extinction model to the reflectance data

After converting the number of layers to mass per area (see Table 1 for values), we fitted the extinction model (Eq. 5) to the measured reflectance data of 1–8 layers of oak leaves and camouflage net. We selected 12 various wavelengths spread between 400–2200 nm at which we fitted the data by adjusting two fitting parameters: the reflectivity (α) and extinction coefficient (k). The wavelengths were chosen based on the reflectance curve of the oak leaves (Fig. 1 (a)), e.g. to center at interesting tops and valleys. The fitting parameters and selected wavelengths are presented in Table 2. In Figure 3 we present the measured sample reflectance plotted against mass per area for the oak leaves (blue squares) and camouflage textile (green circles) at 550, 900, 1270, and 1660 nm. The estimated reflectance values after fitting the model to the data are presented in the same figure (red dashed and black dotted lines).

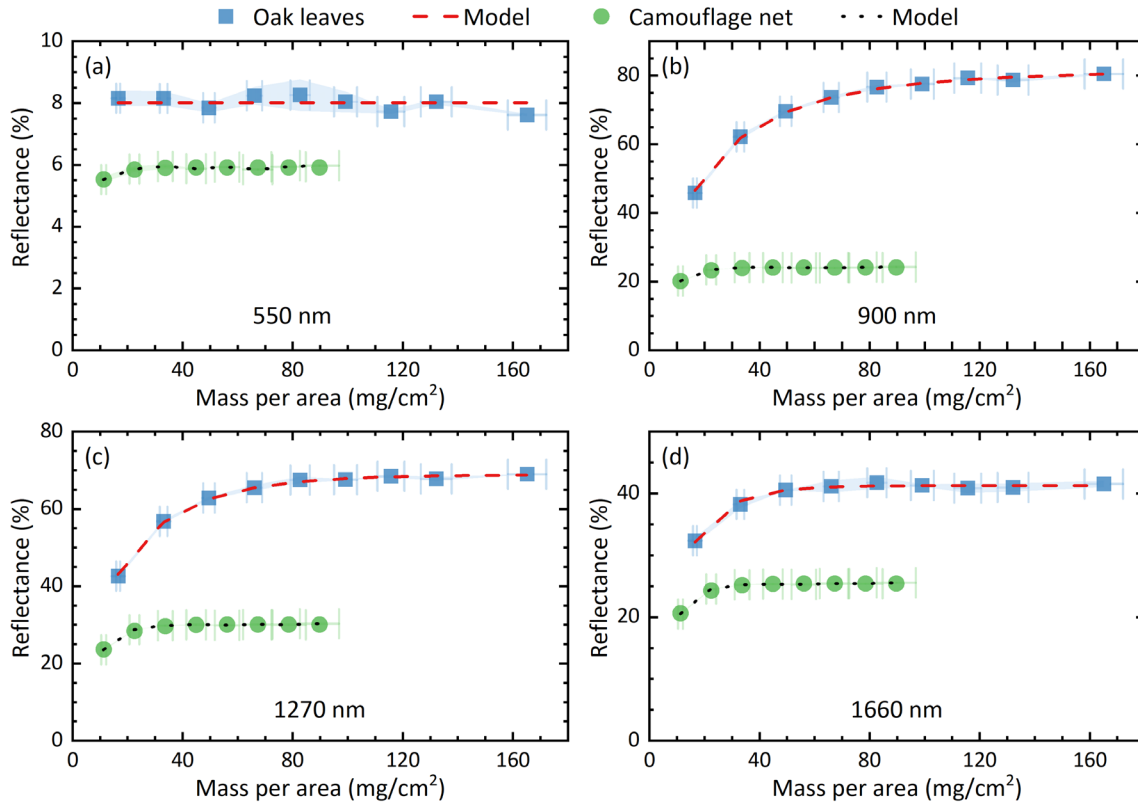


Figure 3. Reflectance plotted against mass per area for oak leaves (blue squares) and camouflage net samples (green circles) at (a) 550 nm, (b) 900 nm, (c) 1270 nm, and (d) 1660 nm. The red dashed lines (oak leaves) and black dotted lines (camouflage net) represent the estimated reflectance from fitting the data with the extinction model. The shaded bands and vertical error bars represent the standard error of the reflectance mean and mass per area mean, respectively (errors smaller than the lines might not be visible in the plot).

At 550 nm (Fig. 3 (a)), the reflectance of both samples is low (close to the background reflectance $\sim 4\%$) and does not change markedly with mass per area. The reflectance changes more at 900 nm (Fig. 3(b)), 1270 nm (Fig. 3(c)) and 1660 nm (Fig. 3(d)), especially for the oak leaf samples (blue squares). At 900 nm, the reflectance of an oak leaf sample increases from $\sim 45\%$ to $\sim 80\%$ when the sample mass per area increases from 17 – 165 mg/cm².

The extinction model (dashed and dotted lines) fits well with the reflectance data at all the selected wavelengths. The reflectivity fitting parameter is similar to the reflectance of the samples at high mass per area values, i.e. the asymptotic reflectance value when the sample thickness goes toward infinity, while the extinction coefficient describes how fast the sample reflectance goes towards the reflectivity value with increased thickness. A high extinction coefficient means that the sample absorbs much of the incoming light and that a small thickness is necessary to hinder reflectance contributions from the background. In other words, a sample with a high extinction coefficient would exhibit a flat reflectance vs. thickness curve. That is why the extinction coefficient from the fitting procedure (Table 2) is high at wavelengths where

the samples exhibited small reflectance variation with thickness, and low at wavelengths where the reflectance changed considerably with thickness. We chose a boundary of 1.0 for the extinction parameter to avoid large numbers for flat reflectance vs. mass per area curves. In Fig. 3, the camouflage net sample has a flatter reflectance curve at 990, 1270, and 1660 nm compared to the oak leaves. Consistently, at these wavelengths, the k -value of the net is larger than that of the leaves (Table 2).

Table 2. Fitting parameters. Reflectance (α) and extinction coefficients (k , unit: cm^2/mg) from fitting the reflectance of oak leaves and camouflage net with the extinction model for various wavelengths (λ) between 400 and 2220 nm. The boundaries of the fitting parameters were set to [0.001, 1.0].

| λ (nm) | α_{oak} | k_{oak} | α_{net} | k_{net} |
|----------------|-----------------------|------------------|-----------------------|------------------|
| 400 | 0.04 | 0.997 | 0.05 | 0.058 |
| 550 | 0.08 | 0.999 | 0.06 | 0.073 |
| 700 | 0.09 | 0.999 | 0.06 | 0.071 |
| 750 | 0.67 | 0.021 | 0.10 | 0.080 |
| 900 | 0.81 | 0.011 | 0.24 | 0.071 |
| 1070 | 0.81 | 0.011 | 0.27 | 0.065 |
| 1270 | 0.69 | 0.018 | 0.30 | 0.059 |
| 1450 | 0.20 | 0.076 | 0.31 | 0.058 |
| 1660 | 0.41 | 0.039 | 0.25 | 0.064 |
| 1840 | 0.35 | 0.045 | 0.31 | 0.056 |
| 1930 | 0.05 | 1.000 | 0.31 | 0.055 |
| 2220 | 0.20 | 0.066 | 0.26 | 0.062 |

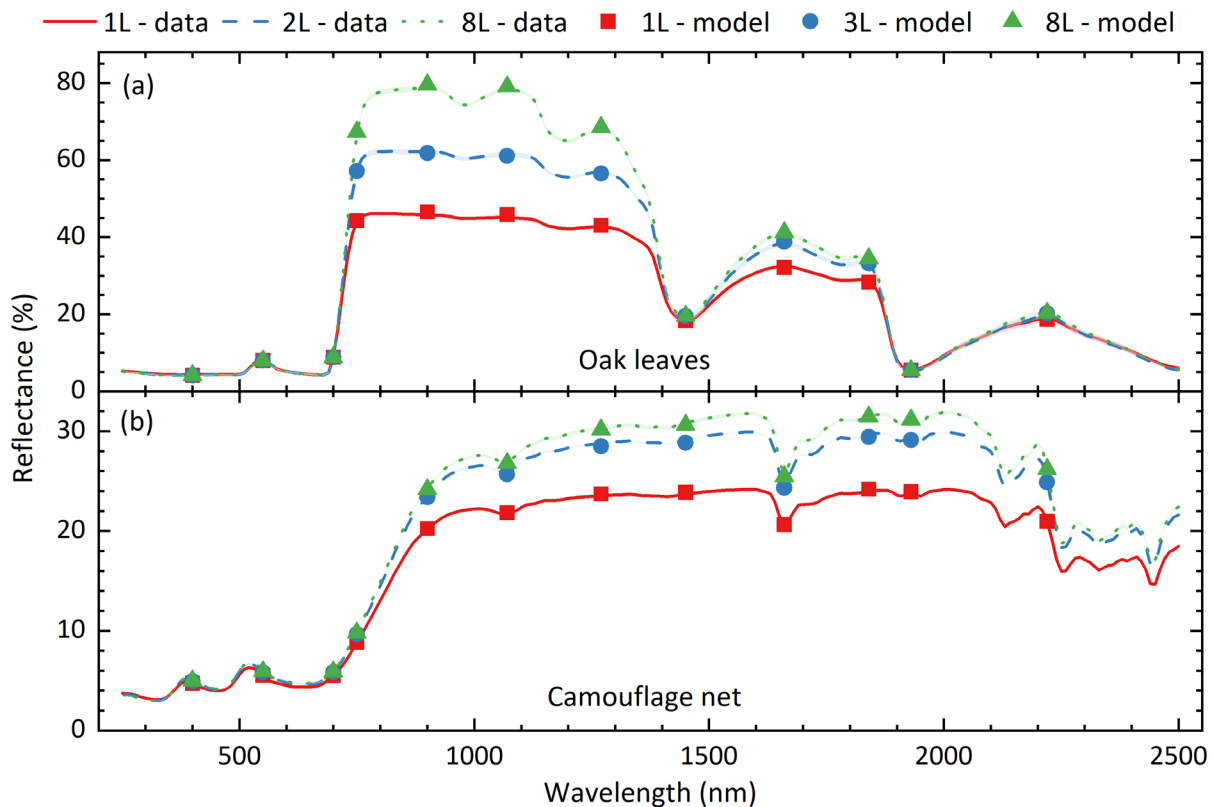


Figure 4. Spectral reflectance measurements of 1 (red lines), 2 (blue dashed lines,) and 8 layers (green dotted lines) of (a) oak leaves and (b) camouflage net between 250 and 2500 nm. The symbols represent estimated reflectance values at selected wavelengths calculated from fitting the measured reflectance data with the extinction model. A black background was used for the reflectance measurements (reflectance between 4–5%). The shaded bands behind the lines represent the standard error of the reflectance mean (errors smaller than the lines might not be visible in the plot).

Figure 4 presents the spectral measurements of 1 (red lines), 2 (blue dashed lines), and 8 layers (green dotted lines) of (a) oak leaves and (b) camouflage net between 250 and 2500 nm together with the estimated reflectance values (square, circle and triangle symbols) from fitting the reflectance data with the extinction model. The figure demonstrates how well the model fits the reflectance data for various sample thicknesses at different wavelengths, including reflectance tops, valleys, and slopes. Samples with 8 different layers (thicknesses) were used for the reflectance fitting, however, it is not necessary to measure and use so many layers if the sample has a high extinction coefficient, i.e. if the measured reflectance value of the sample quickly reaches a constant value when increasing the number of layers. For example, at 550 nm, the reflectance of the oak leaves and camouflage net samples did not change markedly when increasing the number of layers beyond 1–2 layers. At this wavelength, more than 3 layers will not change the fitting parameters significantly. At such conditions, if possible, it would be more useful to measure thinner samples.

5 RESULTS – TRANSMITTANCE

5.1 Transmittance of multiple layered samples

To better understand the spectral properties of the samples, we also measured the transmittance of 1–8 layers of the samples between 250–2500 nm. Figure 5 presents the measured transmittance of 1 (red solid lines), 2 (blue dashed lines), 3 (green dotted lines), 6 (violet dash-dotted lines), and 8 layers (orange dash-dot-dashed lines) of (a) oak leaves and (b) camouflage net samples. The camouflage net transmitted more light than the oak leaves in the UV and VIS wavelength bands, and above ~1350 nm. We found that the transmittance of the leaf samples dropped at wavelengths with high water absorption[50], and had a characteristic transmittance peak around 550 nm where the plant pigments absorb less light[8, 9].

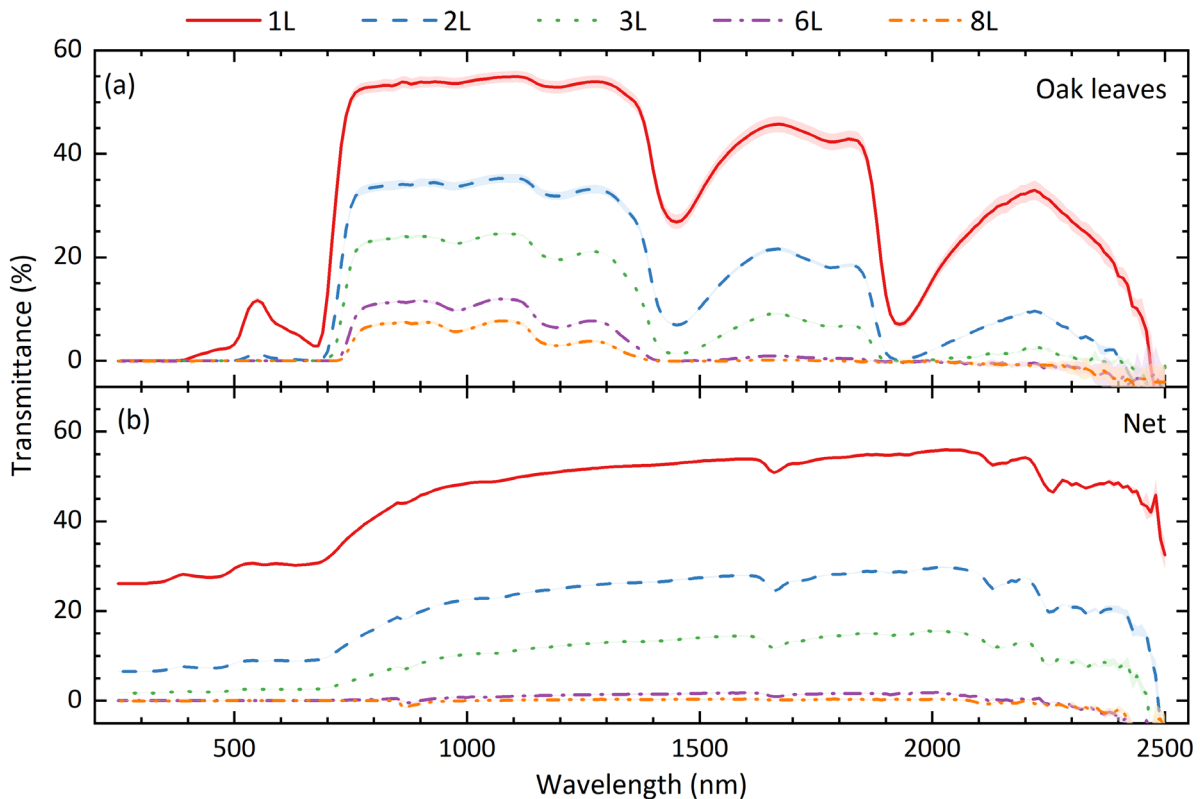


Figure 5. Spectral transmittance measurements of 1 (red solid lines), 2 (blue dashed lines), 3 (green dotted lines), 6 (violet dash-dotted lines), and 8 layers (orange dash-dot-dashed lines) of (a) oak leaves and (b) camouflage net between 250 and 2500 nm. The shaded bands behind the lines represent the standard error of the reflectance mean (errors smaller than the lines might not be visible in the plot).

Below 700 nm and around 1930 nm, the transmittance of the leaf samples with 2 layers was close to zero. For wavelengths longer than 1400 nm, the penetration depth of the leaf samples was 6 layers, while between 700–1400, more than 8 layers were required to block light from transmitting through the sample. The low reflectance (Figure 2) and transmittance of the oak leaf samples below 700 nm (UV and VIS region) and at the longest wavelengths (above 2300 nm) indicates high absorptance at those wavelengths. The absorptance of the samples will be discussed in Sec. 6.

Below 700 nm, the transmittance of the camouflage net approached zero when the thickness was 4 layers (Figure 5 (b)). At longer wavelengths, the penetration depth of the net sample was 6 layers. When considering the effect of the background on the measured reflectance (Fig. 2), the two-way transmittance has to be considered, i.e. the amount of light that transmits through the sample, hits the background, then transmits back through the sample again. As an example, the measured transmittance of 8 layers of oak leaves is lower than 8%. Assuming that the transmittance is the same both ways, the sample's two-way transmittance is less than 0.64% ($0.08^2 \times 100\%$). Because the background reflectance was lower than 5%, the amount of measured reflectance contribution from the background should be less than $0.0064 \times 0.05 \times 100\% = 0.00032\%$. This contribution is so small that it can be neglected, and it is therefore not necessary to measure the reflectance of thicker samples (more layers).

5.2 Comparing estimated and measured transmittance

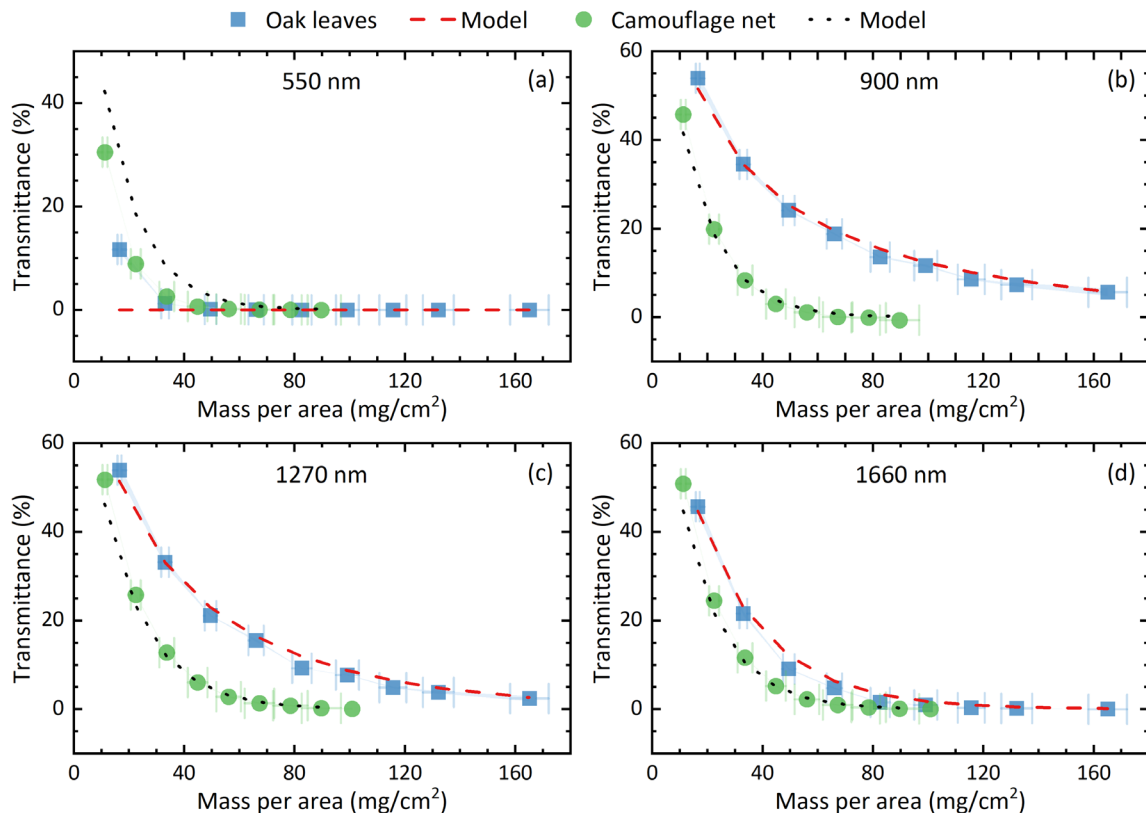


Figure 6. Transmittance plotted against mass per area for oak leaves (blue squares) and camouflage net samples (green circles) at (a) 550 nm, (b) 900 nm, (c) 1270 nm, and (d) 1660 nm. The red dashed lines (oak leaves) and black dotted lines (camouflage net) represent the estimated transmittance from fitting the data with the extinction model. The shaded bands and vertical error bars represent the standard error of the transmittance mean and mass per area mean, respectively (errors smaller than the lines might not be visible in the plot).

Figure 6 shows transmittance data at 550, 900, 1270, and 1660 nm against mass per area. The data is compared with the estimated transmittance (dashed and dotted lines) that was calculated by Eq. 6 and by using reflectivity and extinction coefficient values (Table 2) from fitting the reflectance data (Fig. 2) with the extinction model. The estimated transmittance values were similar to the measured transmittance data, especially at 900, 1270, and 1660 nm. At 550 nm, the model overestimated the transmittance of the thinnest camouflage net samples (mass per area less than ~ 70 mg/cm²,

corresponding to 5 layers) and underestimated the transmittance of the thinnest oak leaf samples (mass per area less than $\sim 40 \text{ mg/cm}^2$, corresponding to 2 layers). We believe that the discrepancy between the model and data at this wavelength is due to the nearly constant reflectance data (Fig. 3 (a)) and errors in the measurements. When the sample reflectance is nearly constant over several sample thicknesses, measurement errors might become more prominent than reflectance differences, hence concealing the true reflectance trends.

At 900, 1270, and 1660 nm, the model slightly underestimated (up to 10%) the transmittance of the thinnest samples (1 layer), while the estimated transmittance of the thicker samples fitted well with the measured transmittance data. We do not have sufficient data to conclude whether the discrepancy was caused by measurement errors or a limitation of the model. Future studies should investigate this by using samples of various thicknesses and densities. To reduce sources of errors, homogeneous samples unaffected by moisture or other time-related changes would then be preferable.

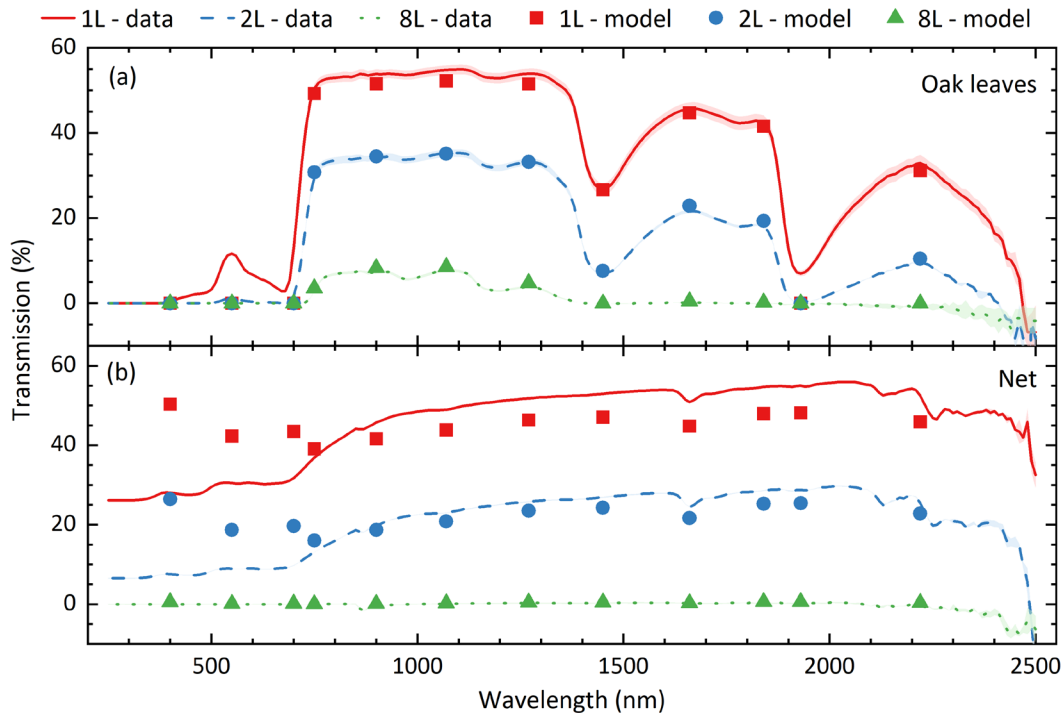


Figure 7. Spectral transmittance measurements of 1 (red lines), 2 (blue dashed lines) and 8 layers (green dotted lines) of (a) oak leaves and (b) camouflage net between 250 and 2500 nm. The symbols represent estimated transmittance values at selected wavelengths calculated from fitting the measured reflectance data with the extinction model. The shaded bands behind the lines represent the standard error of the reflectance mean (errors smaller than the lines might not be visible in the plot).

Figure 7 shows the measured transmittance of 1 (red squares), 2 (blue circles), and 8 layers (green triangles) of the oak leaf and camouflage net samples between 250 and 2500 nm. To understand how well the extinction model estimates the samples' transmittance, the estimated values (dashed and dotted lines) are calculated and added to the figure at selected wavelengths. For the oak leaf samples, the difference between the estimated and measured transmittance values was small. The biggest discrepancy was observed between $\sim 400\text{--}750 \text{ nm}$ where the model underestimated the transmittance. As discussed above, this is likely due to errors in the reflectance measurements (on which the extinction model was used) becoming dominant when the change in reflectance against thickness is small. Discrepancies between the estimated and measured transmittance data were also observed for the camouflage net samples (Figure 7 (b)). The discrepancies were largest for the samples with 1 and 2 layers at wavelengths below 750 nm. That is the wavelength range where the reflectance data of the camouflage net samples collapse on a single reflectance curve (Fig. 2 (b)). For wavelengths longer than 750 nm, the extinction model underestimated the transmittance value of the 1 and 2-layered net samples by up to 12%. Based on our findings, it seems that the extinction model is more accurate when the model is fitted to data that differ considerably with thickness. The reflectance of the camouflage net hardly varied when the sample thickness was larger than 3, i.e. the model had a maximum of 3 data points where the data differed significantly more than the error. For more accuracy of the estimated transmittance, it is therefore better to use the model on thinner or lighter samples.

6 RESULTS – ABSORPTANCE

6.1 Absorptance data

From the reflectance (r) and transmittance (t) measurements, we calculated the absorptance of the samples by using the relationship: $a = 1 - r - t$. Figure 8 presents the absorptance of 1 (red solid lines), 2 (blue dashed lines), 3 (green dotted lines), 6 (violet dash-dotted lines), and 8 layers (orange dash-dot-dashed lines) of oak leaves and camouflage net samples between 250 and 2500 nm. For the oak leaf samples, the absorptance was around 90% below 700 nm, while it dropped to ~0-14% at 800 nm. Below 700 nm, the high absorptance was due to chlorophyll in the leaves[8]. The absorptance then increased with wavelength and revealed some absorptance peaks corresponding to water absorptance lines[50]. These same absorptance peaks were not present for the camouflage net samples (Figure 8 (b)) as they do not contain water. Instead, the net had some prominent absorptance peaks around 1660, 2140, and 2250 nm.

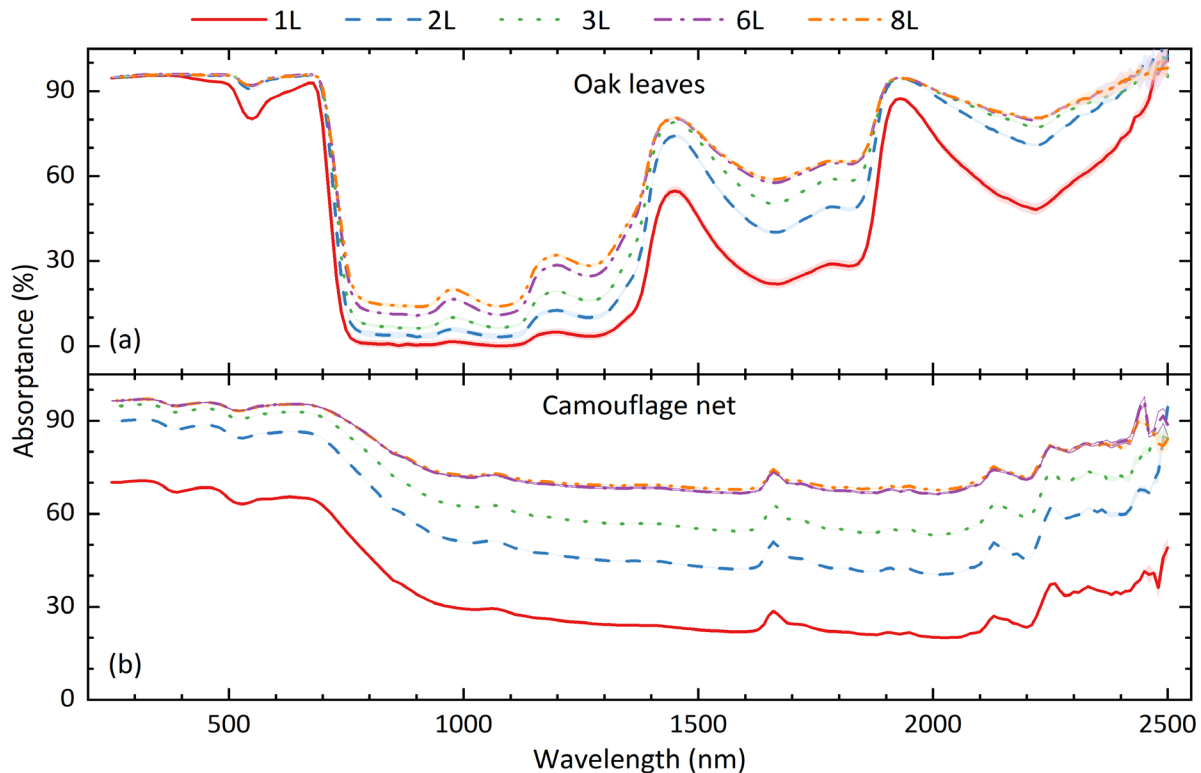


Figure 8. Spectral absorptance of 1 (red solid lines), 2 (blue dashed lines), 3 (green dotted lines), 6 (violet dash-dotted lines), and 8 layers (orange dash-dot-dashed lines) of (a) oak leaves and (b) camouflage net between 250 and 2500 nm. The shaded bands behind the lines represent the standard error of the reflectance mean (errors smaller than the lines might not be visible in the plot).

As expected, the absorptance of both samples greatly increased with the thickness (layers), and the thickness required to saturate the sample absorptance varied with wavelength. For example: 1 layer below 400 nm; 2 layers between 400–720 nm, around 1930 nm, and above 2430 nm; 3 layers around 1450 nm; 8 layers or more between 400 – 1300 nm. For the camouflage net samples, 4 and 6 layers were required to saturate the sample absorptance below and above 700 nm, respectively.

6.2 Comparing estimated and measured absorbance

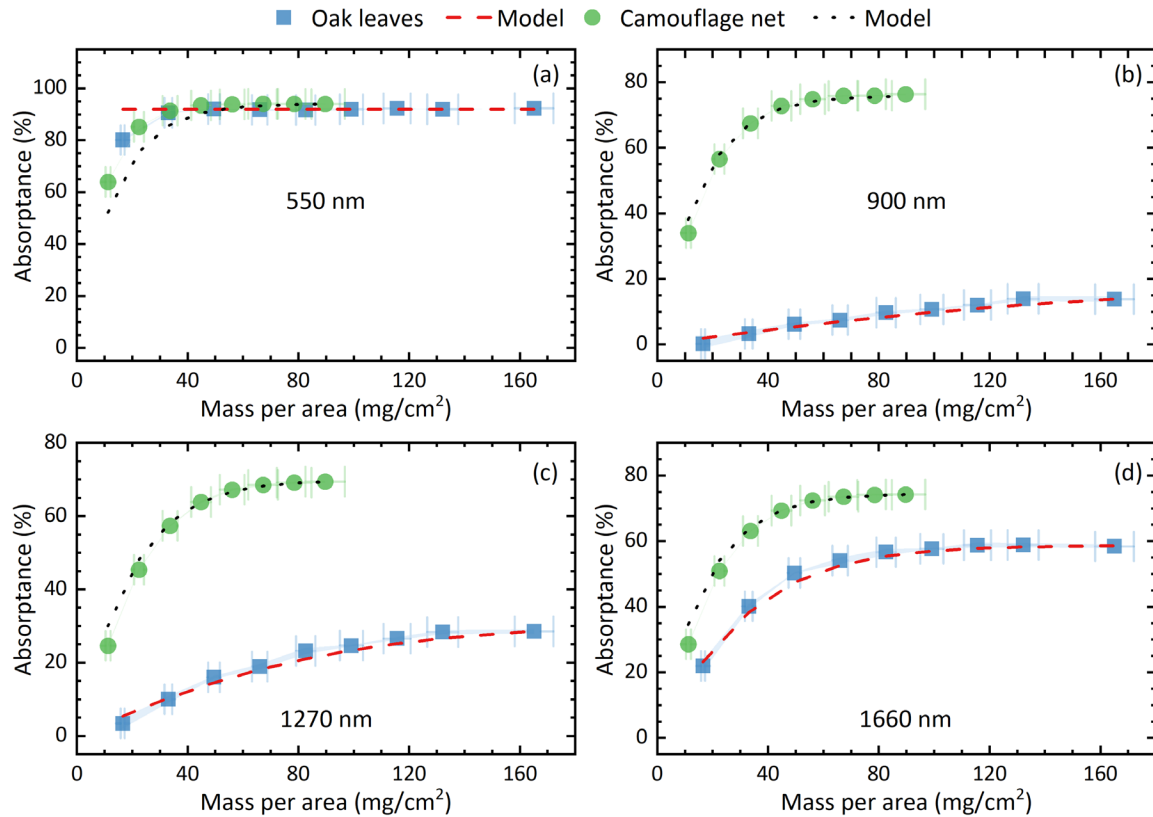


Figure 9. Absorbance plotted against mass per area for oak leaves (blue squares) and camouflage net samples (green circles) at (a) 550 nm, (b) 900 nm, (c) 1270 nm, and (d) 1660 nm. The red dashed lines (oak leaves) and black dotted lines (camouflage net) represent the estimated absorbance from fitting the data with the extinction model. The shaded bands and vertical error bars represent the standard error of the absorbance mean and mass per area mean, respectively (errors smaller than the lines might not be visible in the plot).

We also compared the absorbance data of the samples at selected wavelengths with estimated absorbance values (Fig. 9) calculated by using the extinction model on the measured reflectance data (Fig. 2). The estimated absorbance values fitted well with the data, especially for thicker samples (larger than 2 layers). At 550, 900, 1270, and 1660 nm, the model slightly overestimated the absorbance for the thinnest samples (Fig. 9). The only exception was the estimated absorbance values of the thinnest camouflage samples at 550 nm that were lower than the absorbance data. These discrepancies were expected owing to the estimated reflectance (Fig. 3) and transmittance values at these wavelengths (Fig. 6) and the relationship used for the absorbance $a = 1 - r - t$.

Figure 10 shows the absorbance of the oak leaf and camouflage net samples of 1 (red lines), 2 (blue dashed lines), and 8 layers (green dotted lines) between 250 and 2500 nm together with the estimated absorbance values (symbols) at selected wavelengths between 400 and 2200 nm. Apart from the valley around 550 nm, we found that the estimated absorbance matched the absorbance data of the oak leaves at all the chosen wavelengths and sample thicknesses. For the camouflage net samples with 1 and 2 layers (red squares and blue circles, Figure 10 (b)), the estimated absorbance values were lower than the measured values below 800 nm, and slightly higher than the measured values above 800 nm. The camouflage net sample with 8 layers had similar absorbance at the selected wavelengths (400 – 2200 nm).

Note that the extinction coefficients from fitting the reflectance data of the samples (Fig. 2) with the extinction model were in agreement with the absorbance values of the samples (Fig. 10). The extinction coefficient was high at wavelengths where the samples absorbed a high percentage of the light (per mass density unit), and low at wavelengths with low absorbance. For example, at 400 nm, the extinction coefficient of 1 layer thick oak leaf and camouflage net samples were 0.997 and 0.058, respectively, while their absorbance were 96% and 67%.

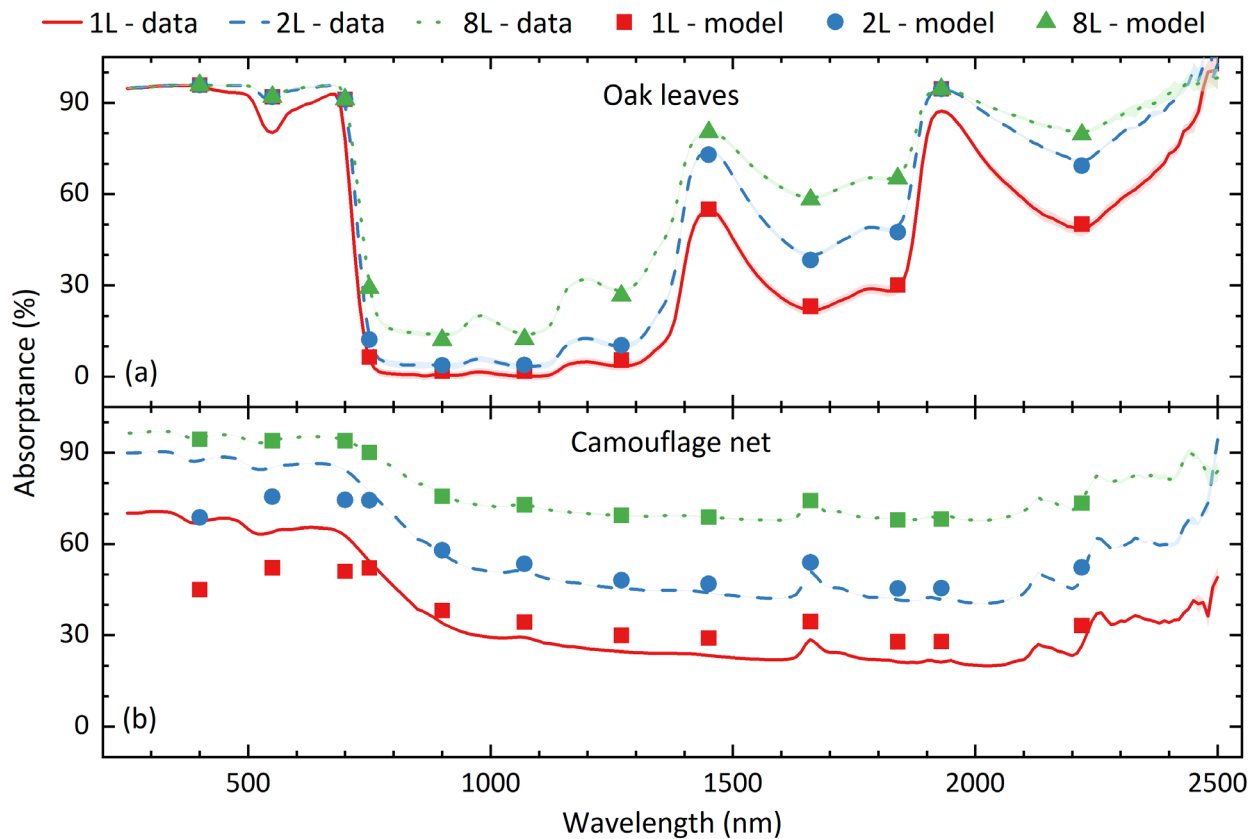


Figure 10. Spectral absorbance measurements of 1 (red lines), 2 (blue dashed lines), and 8 layers (green dotted lines) of (a) oak leaves and (b) camouflage net between 250 and 2500 nm. The symbols represent estimated absorbance values at selected wavelengths calculated from fitting the measured reflectance data with the extinction model. Note that some of the data points (symbols) overlap and are therefore not visible in the plot. The shaded bands behind the lines represent the standard error of the reflectance mean (errors smaller than the lines might not be visible in the plot).

7 CONCLUSIONS AND FUTURE WORK

In this work, we have measured the reflectance and transmittance of layered samples of oak leaves and a generic camouflage net on a black background at wavelengths 250–2500 nm. By measuring samples of different thicknesses, we were able to study how thickness affects the spectral properties of the sample materials. In the UV and visible regions, both the oak leaf and camouflage net samples reflected a small part (less than 8%) of the incoming light, and we observed no significant change in reflectance with sample thickness. Further transmittance measurements revealed that little light was transmitted at these wavelengths, signifying that the samples absorbed most of the UV and visible light. The high absorption was expected for the leaves owing to pigments absorbing light for photosynthesis[8].

We observed that the samples reflected more of the incoming light at NIR and SWIR wavelengths, and there were considerable differences in penetration depth. Between ~800 and 1300 nm, the penetration depth was 6 and 3 layers of the oak leaf and camouflage net samples, respectively. At these wavelengths, we found that the samples transmitted a large portion of the light (up to 55% for a single layer) and hence exhibited low absorbance. From a concealment point of view, these samples (oak leaves or net) have to be thicker to conceal an object exposed to a sensor detecting IR or SWIR wavelengths compared to UV or VIS sensors. Moreover, the camouflage net tested in this study required fewer layers than the oak leaves to conceal the reflectance from an object underneath. However, at certain wavelengths corresponding to water absorption peaks (e.g. 1450 nm), the oak leaf reflectance markedly decreased and 1-2 layers of oak leaves were sufficient to conceal underneath objects.

To compare the samples, we measured their mass per area (Table 1). The mass per area of the oak leaves were ~50% larger than that of the camouflage net, however, the net samples had the highest transmittance compared to the oak leaves. That was probably because the net was perforated. During measurements, there might have been some degree of overlapping holes in the net samples, however, we ensured that this effect was reduced by randomly orienting the net layers between measurements. At selected wavelengths between 400–2200 nm, the measured reflectance of the samples (with thicknesses 1–8 layers) were fitted to a mathematical model named the extinction model. In the model, the layers are modeled as stacked plates with wavelength-dependent reflectivity and energy loss. The energy loss is given by an extinction coefficient k , where e^{-kw} is the remaining energy fraction after absorption in a unit weight per area w of the material. The extinction model fitted the reflectance data accurately at the selected wavelengths. Using the fitting parameters (reflectivity and extinction coefficient, Table 2), we estimated the transmittance and absorptance of the oak leaf and camouflage net samples at the selected wavelengths. At these wavelengths, we compared the estimated values with the measured transmittance and absorptance (measured indirectly) values. We found that the estimated values matched the measured values, especially for the oak leaf samples. The model overestimated the transmittance values of the thinnest camouflage net samples below ~800 nm, and slightly underestimated the values at wavelengths longer than 800 nm, and conversely for the absorptance values. We hypothesize that the model estimated the transmittance and absorptance of the oak leaf samples with higher accuracy than those of the camouflage nets because the reflectance of the leaves provided better data for the model, i.e. more data points where the reflectance changed markedly with thickness.

Overall, the extinction model showed great potential for estimating the transmittance and absorptance values of samples based on a few reflectance measurements, especially if the reflectance of the measured sample changes markedly with thickness. Utilizing the model allows for fewer experiments and can save valuable time and resources. If researchers lack equipment, modeling could also be a useful substitution for spectral measurements. Here we fitted the model to reflectance data, however, it could likewise be fitted to transmittance or absorptance data if more convenient. In contrast to the model utilized in our previous study[25], the extinction model considers multiple reflections between layers and absorption effects. These effects are important for samples with high reflectivity and absorptance. Moreover, the extinction model does not need to be fitted to measurements performed on backgrounds.

Future studies should investigate how the model works when fitted with transmittance or absorptance data, and test samples that are thinner/lighter and with other surface characteristics. It would also be interesting to study samples of different densities, moistures and extend the estimation of spectral values from few selected wavelengths to include all measured wavelengths. In our experiments, we always used a black background. The extinction model should also be tested with samples on different backgrounds, e.g. whiter backgrounds. Another key area for further investigation is the effect of layer spacing on the spectral properties of stacked samples. Layer spacing is an important architectural variable of canopies and can vary significantly depending on the environment.

ACKNOWLEDGMENTS

The works was funded by The Norwegian Defence and Research Establishment (FFI).

The authors have no conflicts of interests.

REFERENCES

- [1] J. A. Endler, [A Predator's View of Animal Color Patterns] Springer US, Boston, MA(1978).
- [2] R. T. Hanlon, C.-C. Chiao, L. M. Mäthger *et al.*, "Cephalopod dynamic camouflage: bridging the continuum between background matching and disruptive coloration," *Philosophical Transactions of the Royal Society B: Biological Sciences*, 364(1516), 429-437 (2009).
- [3] M. Stevens, and S. Merilaita, "Animal camouflage: current issues and new perspectives," *Philosophical Transactions of the Royal Society B: Biological Sciences*, 364(1516), 423-427 (2009).
- [4] R. C. Duarte, A. A. V. Flores, and M. Stevens, "Camouflage through colour change: mechanisms, adaptive value and ecological significance," *Philosophical Transactions of the Royal Society B: Biological Sciences*, 372(1724), 20160342 (2017).
- [5] S. Merilaita, N. E. Scott-Samuel, and I. C. Cuthill, "How camouflage works," *Philosophical Transactions of the Royal Society B: Biological Sciences*, 372(1724), 20160341 (2017).
- [6] L. Talas, R. J. Baddeley, and I. C. Cuthill, "Cultural evolution of military camouflage," *Philosophical Transactions of the Royal Society B: Biological Sciences*, 372(1724), 20160351 (2017).
- [7] J. A. ENDLER, "An overview of the relationships between mimicry and crypsis," *Biological Journal of the Linnean Society*, 16(1), 25-31 (1981).
- [8] D. M. Gates, H. J. Keegan, J. C. Schleter *et al.*, "Spectral properties of plants," *Applied Optics*, 4(1), 11-20 (1965).
- [9] L. Grant, "Diffuse and specular characteristics of leaf reflectance," *Remote Sensing of Environment*, 22(2), 309-322 (1987).
- [10] D. A. Sims, and J. A. Gamon, "Relationships between leaf pigment content and spectral reflectance across a wide range of species, leaf structures and developmental stages," *Remote Sensing of Environment*, 81(2), 337-354 (2002).
- [11] J. R. Miller, J. Wu, M. G. Boyer *et al.*, "Seasonal patterns in leaf reflectance red-edge characteristics," *International Journal of Remote Sensing*, 12(7), 1509-1523 (1991).
- [12] Y. Gao, and H. Ye, "Bionic membrane simulating solar spectrum reflection characteristics of natural leaf," *International Journal of Heat and Mass Transfer*, 114, 115-124 (2017).
- [13] Y. Gao, B. Tang, G. Ji *et al.*, "A camouflage coating with similar solar spectrum reflectance to leaves based on polymeric inorganic composite," *Materials Research Express*, 8(6), 066404 (2021).
- [14] P. Ceccato, N. Gobron, S. Flasse *et al.*, "Designing a spectral index to estimate vegetation water content from remote sensing data: Part 1: Theoretical approach," *Remote Sensing of Environment*, 82(2), 188-197 (2002).
- [15] P. Bowyer, and F. M. Danson, "Sensitivity of spectral reflectance to variation in live fuel moisture content at leaf and canopy level," *Remote Sensing of Environment*, 92(3), 297-308 (2004).
- [16] Q. Jiao, X. Liu, B. Liu *et al.*, "Study on the predicted model of crop leaf water status by the NIR band of ground reflectance and spaceborne hyperspectral images," *Proc. SPIE*, 6835, 68351H (2008).
- [17] C. Proctor, B. Lu, and Y. He, "Determining the absorption coefficients of decay pigments in decomposing monocots," *Remote Sensing of Environment*, 199, 137-153 (2017).
- [18] L. Wang, J. J. Qu, X. Hao *et al.*, "Estimating dry matter content from spectral reflectance for green leaves of different species," *International Journal of Remote Sensing*, 32(22), 7097-7109 (2011).
- [19] G. Cui, J. Hu, C. Jian *et al.*, "Analysis and research on thermal infrared properties and adaptability of the camouflage net," *Proc. SPIE*, 10157, 1015735 (2016).
- [20] G. Selj, and D. Heinrich, "A field-based method for evaluating thermal properties of static and mobile camouflage," *Proc. SPIE*, 10794, 107940B (2018).
- [21] J. Jersblad, and P. Jacobs, "Thermal transmission of camouflage nets revisited," *Proc. SPIE*, 9997, 99970S (2016).
- [22] J. Loyd, and J. Sanders, "Physically realistic camouflage net models for visualization and signature generation," *Proc. SPIE*, 4370, 72-83 (2001).
- [23] H. Dong, J. Wang, Z. Chen *et al.*, "Propagation characteristic of THz wave in camouflage net material," *Proc. SPIE*, 10461, 104611J (2017).
- [24] J. Jersblad, and C. Larsson, "Camouflage effectiveness of static nets in SAR images," *Proc. SPIE*, 9653, 965304 (2015).
- [25] A. Mikkelsen, and G. Selj, "Spectral reflectance and transmission properties of a multi-layered camouflage net: comparison with natural birch leaves and mathematical models," *Proc. SPIE*, 11536, 1153609 (2020).
- [26] H. Kim, J. Choi, K. K. Kim *et al.*, "Biomimetic chameleon soft robot with artificial crypsis and disruptive coloration skin," *Nature Communications*, 12(1), 4658 (2021).

- [27] C. Xu, M. Colorado Escobar, and A. A. Gorodetsky, "Stretchable cephalopod-inspired multimodal camouflage systems," *Advanced Materials*, 32(16), 1905717 (2020).
- [28] L. Huang, S. Ding, Y. Li *et al.*, "Electromagnetic scattering from basic cloth of camouflage net knitted with curved conductive fibers." 241-244.
- [29] S. Brzeziński, T. Rybicki, I. Karbownik *et al.*, "Textile multi-layer systems for protection against electromagnetic radiation," *Fibres & Textiles in Eastern Europe*, 17(2), 66-71 (2009).
- [30] O. Dev, S. Dayal, A. Dubey *et al.*, "Multi-layered textile structure for thermal signature suppression of ground based targets," *Infrared Physics & Technology*, 105, 103175 (2020).
- [31] H. Shen, L. Tu, X. Yan *et al.*, "Obtaining the thermal resistance of air enclosed at the interface of multilayer fabrics by simulation," *Textile Research Journal*, 89(15), 3178-3188 (2019).
- [32] M. Matusiak, "Investigation of the thermal insulation properties of multilayer textiles," *Fibres & Textiles in Eastern Europe*, 14(5), 98-102 (2006).
- [33] M. A. Jahid, J. Hu, and S. Thakur, "Mechanically robust, responsive composite membrane for a thermoregulating textile," *ACS Omega*, 5(8), 3899-3907 (2020).
- [34] L. Peng, B. Su, A. Yu *et al.*, "Review of clothing for thermal management with advanced materials," *Cellulose*, 26(11), 6415-6448 (2019).
- [35] X. Yin, Q. Chen, and N. Pan, "A study and a design criterion for multilayer-structure in perspiration based infrared camouflage," *Experimental Thermal and Fluid Science*, 46, 211-220 (2013).
- [36] P. Zarco-Tejada, "Development of a vegetation fluorescence canopy model," ESA Scientific and Technical Publications Branch, ESTEC, (2005).
- [37] J. B. Féret, A. A. Gitelson, S. D. Noble *et al.*, "PROSPECT-D: Towards modeling leaf optical properties through a complete lifecycle," *Remote Sensing of Environment*, 193, 204-215 (2017).
- [38] G. G. Stokes, "IV. On the intensity of the light reflected from or transmitted through a pile of plates," *Proceedings of the Royal Society of London*, 11, 545-556 (1862).
- [39] P. Kubelka, "Ein Beitrag zur Optik der Farbanstriche (Contribution to the optic of paint)," *Zeitschrift fur technische Physik*, 12, 593-601 (1931).
- [40] P. Kubelka, "New contributions to the optics of intensely light-scattering materials. Part I," *Journal of the Optical Society of America*, 38(5), 448-457 (1948).
- [41] L. B. Tuckerman, "On the intensity of the light reflected from or transmitted through a pile of plates," *Journal of the Optical Society of America*, 37(10), 818-825 (1947).
- [42] D. T. Rampton, and R. W. Grow, "Optical transmission and reflection properties of a pile of lossy plates," *Applied Optics*, 15(9), 2068-2074 (1976).
- [43] W. L. Schaich, G. E. Ewing, and R. L. Karlinsey, "Influence of multiple reflections on transmission through a stack of plates," *Applied Optics*, 45(27), 7012-7017 (2006).
- [44] L. G. Sokoletsky, A. A. Kokhanovsky, and F. Shen, "Comparative analysis of radiative transfer approaches for calculation of diffuse reflectance of plane-parallel light-scattering layers," *Applied Optics*, 52(35), 8471-8483 (2013).
- [45] R. H. Wilhelm, and J. B. Smith, "Transmittance, reflectance, and absorptance of near infrared radiation in textile materials," *Textile Research Journal*, 19(2), 73-88 (1949).
- [46] H. Y. Yang, S. K. Zhu, K. J. Li *et al.*, "Modelling fabric's optical behaviors," *Materials Science Forum*, 575-578, 1266-1271 (2008).
- [47] W. A. Allen, and A. J. Richardson, "Interaction of light with a plant canopy*," *Journal of the Optical Society of America*, 58(8), 1023-1028 (1968).
- [48] O. Lillesaeter, "Spectral reflectance of partly transmitting leaves: Laboratory measurements and mathematical modeling," *Remote Sensing of Environment*, 12(3), 247-254 (1982).
- [49] K. F. Palmer, and D. Williams, "Optical properties of water in the near infrared*," *Journal of the Optical Society of America*, 64(8), 1107-1110 (1974).
- [50] E. R. Hunt, C. S. T. Daughtry, and L. Li, "Feasibility of estimating leaf water content using spectral indices from WorldView-3's near-infrared and shortwave infrared bands," *International Journal of Remote Sensing*, 37(2), 388-402 (2016).